

ORIGINAL RESEARCH ARTICLE

The most significant brain regions implicated in olfactory dysfunction in Parkinson's disease

Naser Moradi¹, Siamak Shahidi^{2*}, Bahareh Zaker Harofteh^{3**},
 Mohammad Ahmadpanah⁴, Sajjad Farashi², and Ghodrattollah Roshanaei⁵

¹Department of Neuroscience, School of Science and Advanced Technologies in Medicine, Hamadan University of Medical Sciences, Hamadan, Iran

²Neurophysiology Research Center, Institute of Neuroscience and Mental Health, Avicenna Health Research Institute, Hamadan University of Medical Sciences, Hamadan, Iran

³Department of Neurological Disease, Shahid Beheshti University of Medical Sciences, Tehran, Iran

⁴Behavioral Disorders and Substance Abuse Research Center, Institute of Neuroscience and Mental Health, Avicenna Health Research Institute, Hamadan University of Medical Sciences, Hamadan, Iran

⁵Department of Biostatistics, School of Medicine, Arak University of Medical Sciences, Arak, Iran

Abstract

Olfactory dysfunction is observed in over 95% of patients with Parkinson's disease (PD). This study examines the relationship between gray matter volume (GMV) and olfactory impairment in a cohort of 182 subjects, including PD patients and healthy controls (HCs). Using the Iran Smell Identification Test, which is a standardized 24-item olfactory identification assessment, to evaluate the olfactory performance, PD patients were divided into two groups (scores ranging from 0 to 18 indicate olfactory dysfunction, while scores from 19 to 24 indicate normal olfaction): those with normal smell (PD-NS, $n = 23$) and those with smell disorders (PD-SD, $n = 69$). Differences in GMV were analyzed using voxel-based morphometry. Statistical analysis was conducted using SPSS 26. The results revealed that the PD-NS group exhibited reduced GMV in the right thalamus and the left parahippocampal gyrus compared to the HCs. Furthermore, the HC group demonstrated no statistically significant olfactory dysfunction. In contrast, the PD-SD group showed significant decreases in GMV in the right entorhinal cortex and both the right and left hippocampus compared to both the HC and PD-NS groups. These findings indicate that PD patients experience more severe olfactory dysfunction in hippocampal regions than the HC group, likely attributed to the initial pathological loss of gray matter in both the right and left hippocampus.

Keywords: Parkinson's disease; Smell; Gray matter; MRI; Brain volumetry

***Corresponding authors:**

Siamak Shahidi
 (n.moradi@edu.umsha.ac.ir)
 Bahareh Zaker Harofteh
 (bahar.zaker.h@gmail.com)

Citation: Moradi N, Shahidi S, Harofteh BZ, Ahmadpanah M, Farashi S, Roshanaei G. The most significant brain regions implicated in olfactory dysfunction in Parkinson's disease. *Adv Neuro.* 2025;4(3):60-69.
 doi: 10.36922/AN025110024

Received: March 16, 2025

Revised: April 12, 2025

Accepted: April 17, 2025

Published online: May 20, 2025

Copyright: © 2025 Author(s). This is an Open-Access article distributed under the terms of the Creative Commons Attribution License, permitting distribution, and reproduction in any medium, provided the original work is properly cited.

Publisher's Note: AccScience Publishing remains neutral with regard to jurisdictional claims in published maps and institutional affiliations.

1. Introduction

Parkinson's disease (PD) is a chronic and progressive neurodegenerative condition that predominantly affects the dopamine-producing neurons in the substantia nigra, resulting in the development of motor symptoms.¹ PD is acknowledged as a multifaceted condition that impacts various systems and is marked by a range of both motor and non-motor symptoms, including deficits in olfaction. Among the non-motor symptoms

associated with PD, olfactory dysfunction is one of the most prevalent.¹⁻³

Studies have shown that over 95% of individuals with PD experience a notable decline in olfactory function, which can have a significant impact on their daily lives. Unfortunately, the importance of olfaction in enhancing the quality of life and the capacity to derive pleasure is frequently overlooked.^{4,5} Onset age, therapeutic intervention, treatment duration, and disease severity do not have an impact on olfactory dysfunction.^{1,6,7}

Neural responses to olfactory stimuli are transmitted from the nasal epithelium to the olfactory bulb, then to the olfactory cortex along with its primary connections within the brain.^{8,9} The anterior olfactory nucleus, olfactory tubercle, pyriform cortex, amygdala, and entorhinal cortex comprise the olfactory cortex, each receiving input from neurons in the olfactory bulb. The pyriform cortex, divided into anterior and posterior segments, serves as the primary output region for projections from the olfactory bulb. Odorant identity is encoded in the anterior pyriform cortex, while the posterior pyriform cortex encodes odor quality.¹⁰ The entorhinal cortex is connected to the hippocampus, and its dysfunction can have an impact on the ability to remember and distinguish between different odors.^{11,12} The orbitofrontal cortex represents a significant olfactory pathway extending beyond the olfactory cortex. Despite its importance, the precise function of this brain region in olfaction remains unclear. Studies have linked it to tasks such as distinguishing between different odors, recognizing smells, and regulating olfactory attention.¹³⁻¹⁵ Lewy bodies have been observed in the olfactory bulb, entorhinal cortex, and pyriform cortex during post-mortem examinations of individuals with PD.^{14,15}

The present study aims to investigate the relationship between olfactory dysfunction and gray matter volume (GMV) using voxel-based morphometry (VBM). VBM is capable of examining and assessing the structural alterations in brain areas affected by neurodegenerative disorders, such as dementia, PD, and multiple sclerosis.¹⁶⁻¹⁸ The software (Computational Anatomy Toolbox [CAT], Structural Brain Mapping Group, Germany) was initially suggested and adopted as the norm by Ashburner and Friston¹⁹ VBM automatically assesses the volume of each voxel within the segmented tissues to detect differences that suggest gray matter (GM) atrophy or localized alterations in white matter (WM) density. Consequently, VBM remains impartial regarding structural changes in specific brain regions, circumventing subjective variations introduced by the artificial delineation of regions of interest. It offers an objective and thorough assessment of anatomical changes throughout the entire brain, capable

of detecting even minor variations in brain volume or density.²⁰⁻²³

The goal of this study is to explore the relationship between olfactory dysfunction and GMV in PD, with a focus on comparing individuals with and without olfactory dysfunction.

2. Materials and methods

2.1. Subjects

This study was conducted on 182 subjects, including 92 patients with PD (23 with normal smell [PD-NS] and 69 with smell disorder [PD-SD]) and 90 healthy controls [HCs] from July 29, 2024, to December 13, 2024. A 3-week interval separated the first study visit and the follow-up visit. Informed consent was obtained from all subjects.

The exclusion criteria were as follows: individuals diagnosed with various neurological conditions (e.g., stroke), Parkinsonism syndromes (e.g., progressive supranuclear palsy, multiple system atrophy, and uncommon motor and non-motor symptoms), psychological disorders (e.g., severe depression), individuals for whom magnetic resonance imaging (MRI)'s results were contraindicated, and cases in which any form of artifact on MRI hindered accurate volumetric analysis.

The HCs did not exhibit any neurological conditions, such as stroke, brain tumors, or severe mental disorders. Furthermore, they reported no cognitive complaints.

To control for potential confounding effects of age, gender, and educational level on the outcomes, participants in the HC group were meticulously matched with those in the PD groups based on these covariate variables. To minimize potential confounders, such as cognitive status and medication, the cognitive status of the patients was evaluated using the Montreal Cognitive Assessment, and no significant differences were found between the two groups. In addition, only the *L*-dopa-carbidopa combination treatment was used for the patients in this study, and the effect of this variable is similar in both groups.

2.2. Olfactory assessments

In the present study, the Iran Smell Identification Test (ISIT), a standard 24-item odor identification test, was used to evaluate the olfactory performance of PD and HC groups according to cultural adaptation. A score of 0 to 18 in this test indicates a smell disorder, while 19 to 24 indicates normal smell.²⁴ Baseline demographic and clinical data, including age, gender, educational level, and disease duration, were documented. To develop the ISIT, researchers adapted the University of Pennsylvania Smell Identification Test (UPSIT) for the Iranian population.

Given Iran's diverse ethnicities, the goal was to identify odors familiar to all Iranians. A group of 90 students from various cultural backgrounds residing in Tehran dormitories was asked to review the 40 odors included in the UPSIT and identify those most familiar. To ensure better linguistic comprehension, the original UPSIT was translated into Farsi, and participants were asked to suggest local odors commonly encountered in different regions of Iran. The development of ISIT involved the following steps:

- (i). Identifying and replacing unfamiliar odors.
- (ii). Compiling a preliminary list of 40 odorants, which included both natural and synthetic options, while also producing fragrance microcapsules when necessary.
- (iii). Designing scratch-and-sniff stickers by mixing microcapsules with varnish ink and printing them using a silk screen printer on sticker paper.

A pilot study was then conducted with 43 participants (23 females and 20 males, aged 20 – 40) using this initial version of ISIT. The pilot study aimed to identify any deficiencies in the procedure and to select the most appropriate odors among the 40 items and their alternatives.²⁴

2.3. VBM pre-processing

Preprocessing analysis for VBM was performed using the CAT12 toolbox²⁵ on high-resolution T1-weighted structural images, acquired from all patients on a 1.5 Tesla MRI scanner (Avanto, Siemens Healthineers, Germany), within the Statistical Parametric Mapping (SPM12) framework developed by the Department of Imaging Neuroscience Group (<http://www.fil.ion.ucl.ac.uk/spm>). This analysis was conducted using MATLAB R2023b software (CAT, Structural Brain Mapping Group, Germany). Initially, the anatomical images were segmented into GM, WM, and cerebrospinal fluid using the unified segmentation module.²⁶ After segmentation, the GM images were normalized to the Montreal Neurological Institute (MNI) standard space using the diffeomorphic anatomical registration through exponentiated lie algebra (DARTEL) algorithm.²⁷ Following the affine and non-linear registration of the GM templates in MNI space, the images were modulated to preserve the relative GMVs post-spatial normalization. The resulting GM images were then smoothed with a Gaussian kernel featuring a full width at half maximum of 10 mm. In summary, a VBM analysis comprises the following steps:

- (i) Pre-processing: T1 images are normalized to a template space and segmented into GM, WM, and cerebrospinal fluid. The pre-processing parameters can be adjusted through the module "Segment Data." After the pre-processing is finished, a quality check is highly recommended. This can be achieved through

the modules "Display slices" and "Check sample." Both options are located in the CAT12 window under "Check Data Quality." Furthermore, quality parameters are estimated and saved in XML files for each dataset during pre-processing. These quality parameters are also printed on the report PDF page and can be used in the module "Check sample." Before inputting the GM images into a statistical model, the image data needs to be smoothed.

- (ii) Statistical analysis: The smoothed GM images are input into a statistical model. This requires building a statistical model (e.g., *t*-tests, analysis of variance (ANOVAs), and multiple regressions). This is done by the standard SPM modules "Specify 2nd Level" or preferably "Basic Models" in the CAT12 window, covering the same function but providing additional options and a simpler interface optimized for structural data. The statistical model is estimated. This is done with the standard SPM module "Estimate" (except for surface-based data, where the function "Estimate Surface Models" should be used instead). If total intracranial volume (TIV) is used as a confound in a model to correct for different brain sizes, it is necessary to check whether TIV reveals a considerable correlation with any other parameter of interest, and rather uses global scaling as an alternative approach. After estimating the statistical model, contrasts are defined to get the results of the analysis. This is done with the standard SPM module "Results."^{25,26}

2.4. MRI data acquisition

All patients underwent MRI scans using a 1.5T MRI scanner. The choice of a 1.5T scanner is based on its widespread availability and effectiveness in clinical settings for a variety of neurological assessments. This model has been well-studied and is known for providing high-quality images while maintaining patient comfort.

The scans were performed utilizing the HE1_4 coil element, specifically designed for this scanner. Coil elements play a crucial role in MRI examinations, as they determine the sensitivity of the MRI equipment to the magnetic fields produced by the scanned tissues. The HE1_4 coil element is optimized for head imaging, resulting in an improved signal-to-noise ratio and enhancing the clarity and resolution of the images captured. This optimization is essential for accurately visualizing fine anatomical details and potential pathological changes in brain structures.

To ensure patient comfort and minimize movement during the scanning process, all participants were instructed to lie supine on the MRI table. This position helps in achieving a stable and reproducible imaging setup,

which is critical for consistent results across all scans. In addition, earplugs were provided to reduce the effects of excessive scanner noise, which often reaches levels that can be uncomfortable for patients. The loud sounds produced during MRI scanning can lead to anxiety and involuntary movements, potentially compromising image quality. By using earplugs, we aimed to enhance patient comfort and cooperation during the procedure.

To further enhance stability during the MRI session, firm foam pads were used around the patient's head. These pads served to restrict movement and help maintain the participants' heads in a fixed position, which is vital for acquiring high-quality images. Even slight head movements can result in image blurring, making it difficult to analyze the resultant data accurately. The use of these foam pads, therefore, contributes significantly to the overall quality of the imaging process.

The MRI sequences utilized in this study included T1-weighted images, which are particularly effective for assessing anatomical structures within the brain. T1-weighted imaging is optimal for visualizing GM, WM, and the overall structure of the brain. The imaging parameters for the T1 sequences were set to a voxel size of 1.2 mm × 1.0 mm × 5.5 mm, which allows for a balance between spatial resolution and acquisition efficiency. This voxel size enables the differentiation of various brain tissues while ensuring that the scan duration remains manageable for patients.

The repetition time was set to 426 ms, and the echo time was maintained at 8.7 ms, settings that are widely recognized in the literature for producing high-quality T1-weighted images. These parameters were carefully selected to optimize the contrast between different types of brain tissue, enhancing the visibility of anatomical details essential for both clinical assessment and research analysis.

In summary, the meticulous attention to the MRI acquisition protocol, including the choice of scanner, coil element, patient positioning, noise reduction strategies, and specific imaging parameters, underscores our commitment to obtaining high-quality imaging data that is essential for subsequent analyses and interpretations.

2.5. Statistical analysis

Statistical analysis was performed using version 24.0 of the Statistical Package for the Social Sciences (SPSS, IBM Corporation, USA) software. The paired- and independent-samples *t*-test were utilized to assess the difference in means between two distinct groups. The utilization of one-way ANOVA allowed for the examination of the discrepancies in GMV across the different PD groups and the comparison of average ISIT test scores. Categorical

variables were analyzed through the chi-squared test. The Spearman correlation coefficient was employed to assess the association between the variables. A $p < 0.05$ was deemed statistically significant.

3. Results

3.1. Characteristics of the participants

The analysis included a total of 23 PD-NS, 69 PD-SD, and 92 HCs. The demographic and clinical profiles of these three groups are detailed in Table 1. Age and gender exhibited no significant differences between the HC and PD groups ($p > 0.05$). No significant difference was observed in disease duration, medication administration status, educational level, and disease severity (between PD-NS and PD-SD) ($p > 0.05$). The results of the ISIT tests exhibited strong and significant differences between the means of the HC and PD groups. The ISIT scores for HC, PD-NS, and PD-SD, respectively, are 21.50, 19.50, and 11.40 ($p < 0.001$).

The present study also compared the mean scores for drug types, family history (PD patients with first-degree relatives affected by the disease), first sign of the disease, smoking status, accommodation status, the Montreal Cognitive Assessment, blood types, and weights among the PD groups, revealing no significant differences between the groups ($p > 0.05$).

3.2. Comparison of the GMV between the PD patient with normal smell group and the HC group

The comparison of the mean GMV in the brain of the participants in the PD-NS and HC groups demonstrated a significantly decreased volume within the right thalamus and parahippocampal gyrus of the PD-NS group compared to the HC group (Table 2 and Figure 1).

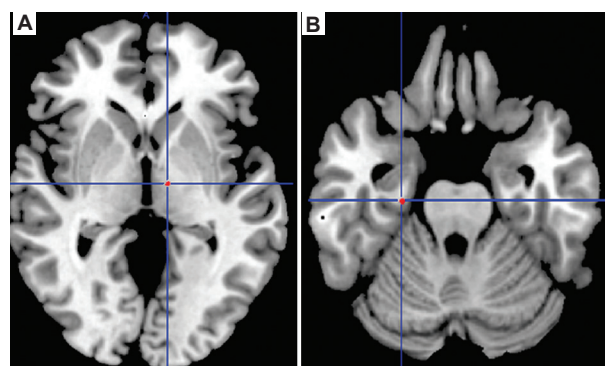


Figure 1. The magnetic resonance imaging scanning of the brain of the participant from the Parkinson's disease patient with normal smell (PD-NS) group. (A) Right thalamus. (B) Left parahippocampal gyrus. The red dots indicate the Montreal Neurological Institute coordinates and a significant reduction in gray matter volume in the PD-NS's brain compared to the healthy control group's brain.

Table 1. Clinical and demographic characteristics of the healthy control (HC), Parkinson's disease patient with normal smell (PD-NS), and PD patients with smell disorder (PD-SD) groups

| Characteristics | PD-NS (n=23) | PD-SD (n=69) | HC (n=90) | p-value |
|--|--------------|--------------|-------------|----------------------|
| Age (years) | 61.09±10.35 | 62.32±10.76 | 60.83±10.07 | 0.445 ^a |
| Gender (male/female) | 14/9 | 40/29 | 53/37 | 0.432 ^b |
| Educational level (years) | 4.18±1.42 | 3.30±1.22 | 3.31±1.49 | 0.390 ^a |
| Disease severity ^d | 2.62±1.03 | 3.17±1.05 | - | 0.036 ^c |
| Disease duration (years) | 4.87±3.16 | 5.47±3.01 | - | 0.550 ^c |
| Medication administration status ^e | 1.25±0.32 | 1.18±0.38 | - | 0.552 ^c |
| ISIT scores | 19.50±1.16 | 11.40±1.30 | 21.50±1.16 | <0.001 ^{a*} |
| Type of used drugs (L-dopa-carbidopa) ^f | 21/2 | 64/5 | - | 0.439 ^b |
| Pharmacological treatment (years) | 4.1±1.12 | 4.3±1.19 | - | 0.419 |
| Smoker (+/-) | 3/20 | 4/65 | - | 0.772 ^b |
| Accommodation status (metropolis/town) | 8/15 | 19/50 | - | 0.390 ^b |
| Family history (+/-) ^g | 2/21 | 7/62 | 1/89 | 0.590 ^b |
| First sign of the disease ^h | i | i | - | 0.213 ^b |
| MoCA scores | 24.34±1.26 | 24.07±1.63 | - | 0.370 ^c |
| Blood types | i | i | i | 0.872 ^b |
| Weight | i | i | i | 0.654 ^b |

Notes: Data are expressed as mean±standard deviation or number; * $p < 0.05$; ^aOne-way ANOVA; ^bChi-squared test; ^cIndependent samples t-test; ^dThis is the disease severity based on the Modified Hoehn and Yahr Scale; ^eThis is the number of medications the patients are taking; ^fL-dopa-carbidopa combination treatment of 250/25 mg or 100/25 mg one tablet every 4 h; ^gPD patients who have first-degree relatives affected by PD; ^hThe onset of the first symptoms of PD with tremor, rigidity, or bradykinesia. For the clinical presentation of PD at the onset of the disease, all patients exhibited asymmetric tremors in the upper limbs, and at the time of enrollment, they presented with tremors, rigidity, and bradykinesia, scoring between 1 and 3 on the Hoehn and Yahr scale. ⁱData not presented in this table due to the presence of multiple categorical values.

Abbreviations: ANOVA: Analysis of variance; ISIT: Iran Smell Identification Test; MoCA: Montreal Cognitive Assessment.

Table 2. Comparison of the mean gray matter volume between the Parkinson's disease patient with normal smell (PD-NS) group and the healthy control (HC) group

| Brain region | PD-NS (n=16) | HC (n=90) | p-value |
|----------------------------|--------------|-----------|---------|
| Right thalamus | 5.35±1.39 | 5.86±1.50 | 0.021* |
| Left parahippocampal gyrus | 3.27±1.01 | 3.99±1.10 | 0.009* |

Notes: Data expressed as mean±standard deviation; Statistical comparisons were conducted using paired-samples *t*-test; * $p < 0.05$.

3.3. GMV between the PD patient with normal smell group and the PD patient with smell disorder group

The comparison of the mean GMV between the brains from the PD-NS group and those from the PD-SD group demonstrated a significantly decreased volume within the right entorhinal cortex, right hippocampus, and left hippocampus of the PD-SD group compared to the PD-NS group (Table 3 and Figure 2).

3.4. Comparison of the GMV between the PD patient with smell disorder group and the HC group

The comparison of the mean GMV between the brains from the HC group and those from the PD-SD group

demonstrated a significantly decreased volume within the right entorhinal cortex, right hippocampus, and left hippocampus of the PD-SD group compared to the HC group (Table 4 and Figure 2).

4. Discussion

The present study investigated the structural changes of the cortical and subcortical regions in PD with and without olfactory dysfunction compared to the HC group. The findings revealed that individuals with PD and olfactory dysfunction had a reduction in the volume of both the right and left hippocampi and entorhinal cortex in comparison to those in the PD-NS and HC groups. In addition, the PD-NS group demonstrated a decrease in the volume of the right thalamus and left parahippocampal gyrus. These results align with findings from previous studies.²⁸⁻³⁰

As a primary olfactory cortex, the entorhinal cortex is vital for processing olfactory signals originating from the olfactory bulb.³¹ Lewy bodies initially emerge in the olfactory nerves. Notably, they are also present in the primary olfactory cortex in the early phase of PD. Their presence may contribute to olfactory dysfunction.³²⁻³⁴ In addition, it serves as a “gateway” for sensory information

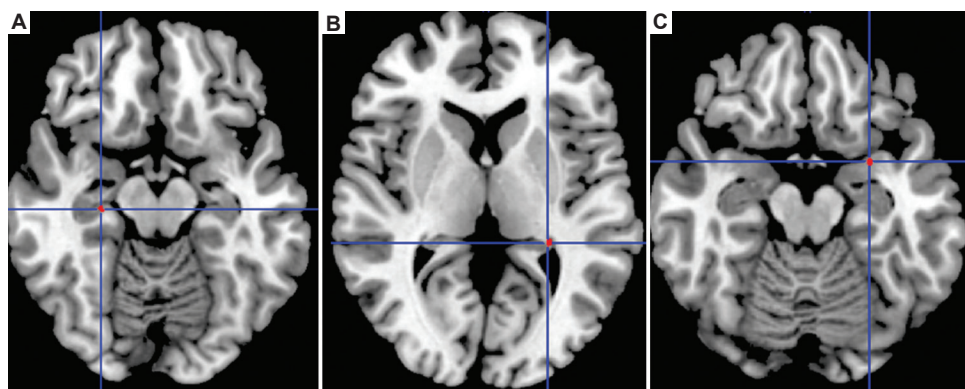


Figure 2. The magnetic resonance imaging scanning of the brain of the participant from the Parkinson's disease patient with smell disorder (PD-SD) group. (A) Left hippocampus. (B) Right hippocampus. (C) Right entorhinal cortex. The red dots indicate the Montreal Neurological Institute coordinates and a significant reduction in gray matter volume in the PD-SD's brain compared to the PD patient with normal smell group's brain.

Table 3. Comparison of the mean gray matter volume between the Parkinson's disease patient with normal smell (PD-NS) group and the PD patients with smell disorder (PD-SD) group

| Brain region | PD-NS (n=23) | PD-SD (n=69) | p-value |
|-------------------------|--------------|--------------|---------|
| Right entorhinal cortex | 2.25±1.00 | 1.91±1.02 | <0.001* |
| Left hippocampus | 2.33±1.10 | 1.84±1.08 | <0.001* |
| Right hippocampus | 2.36±1.17 | 1.85±1.20 | <0.001* |

Notes: Data are expressed as mean±standard deviation or number; Statistical comparisons were conducted using paired-samples *t*-test; **p*<0.05.

Table 4. Comparison of the mean gray matter volume between the Parkinson's disease patient with smell disorder (PD-SD) group and the healthy control (HC) group

| Brain region | PD-SD (n=69) | HC (n=90) | p-value |
|-------------------------|--------------|-----------|---------|
| Right entorhinal cortex | 1.91±1.01 | 2.19±1.11 | <0.001* |
| Left hippocampus | 1.84±1.04 | 2.36±1.45 | <0.001* |
| Right hippocampus | 1.85±1.40 | 2.15±1.05 | <0.001* |

Notes: Data are expressed as mean±standard deviation; Statistical comparisons were conducted using paired-samples *t*-test; **p*<0.05.

from various cortical areas to access the hippocampus. Recent research indicated that the direct circuit from the lateral entorhinal cortex to the hippocampal CA1 is essential for olfactory associative learning.³⁵ In this study, the GMV of the entorhinal cortex in the PD-SD group was lower than that in the other groups. These findings align with pathological research suggesting that the entorhinal cortex may be one of the earliest brain regions affected by PD. Another finding of this study is that both the right and left hippocampi exhibited a significant positive correlation with olfactory dysfunction in PD patients. This indicates that a reduction in bilateral hippocampal volume is associated with olfactory deficits in these individuals.

Selective hyposmia in PD exhibits a stronger correlation with hippocampal dopamine innervation than with that of the amygdala, ventral striatum, or dorsal striatum, as evidenced by diffusion tensor imaging. These results suggest that the mesolimbic dopamine innervation of the hippocampus may play a crucial role in the development of selective hyposmia in PD.³⁶ Recent studies on the hippocampus emphasize that this structure may play a more significant role in olfaction.^{37,38}

Based on the findings of the present study, one can infer the role of the structural network between the entorhinal cortex and the amygdala in PD patients.²³ The entorhinal cortex and the hippocampus have significant connections with each other, and a distortion in these connections may disrupt the olfactory process in the patients. Furthermore, the reduction in brain structure volume can be an important factor alongside the decrease in WM volume, ultimately leading to functional impairments.^{23,39,40}

Neuroimaging research has demonstrated that pathological alterations during aging initiate in the amygdala and hippocampus, particularly in the parahippocampus and entorhinal cortex, which play a crucial role in the recognition and identification of olfactory stimuli.⁴¹ Research showed that a decrease in olfactory function, occurring independently of cognitive decline, was associated with reductions in the volumes of the left hippocampus and left parahippocampus.⁴² Another study demonstrated that a decrease in the volume of the entorhinal cortex was not directly linked to a reduction in olfactory function. Instead, the reduction in entorhinal cortex volume correlated with a decrease in the volume of the parahippocampus, suggesting that the entorhinal cortex influences olfactory ability indirectly through its relationship with the parahippocampus.^{41,43,44} Based on the studies at the WM and cellular levels,⁴⁵ as well as the

structural findings in this study, we conclude that the structural connectivity between the entorhinal cortex and parahippocampal regions plays a crucial role in olfactory function. In PD patients, the reduction of volumes in these areas may have a more significant impact on the olfactory dysfunction.

Another factor that may influence a VBM study is the type of treatment that can influence the morphologic features of the VBM. For example, the study by Donzuso *et al.*⁴⁶ investigated whether a neuroanatomical substrate might underlie the development of long-duration responses using structural MRI and VBM analyses. Their study showed that some cortical structural changes may predispose individual patients to developing long-duration responses to *L*-dopa. Based on the results of the present study, it can be concluded that the type of treatment, along with other factors, such as olfactory dysfunction and the presence of cognitive impairment (mild/moderate/severe), may influence the morphologic features of the VBM.²³ Furthermore, the brain regions exhibiting reduced volume in PD patients undergoing *L*-dopa treatment, with or without olfactory dysfunction, differ from those affected in PD patients with cognitive impairment. Future studies should focus on the effects of medication on brain volumetric results in PD patients. Accounting for comorbid disorders, such as cognitive impairment and olfactory dysfunction, may offer valuable insights.

Moreover, the interplay between pharmacotherapy and neuroanatomical changes may be further elucidated by investigating the underlying biological mechanisms influenced by *L*-dopa treatment. Research indicates that neuroinflammation and dopaminergic signaling alterations can affect neuroplasticity and neurodegeneration in PD.⁴⁷⁻⁴⁹ Studies employing advanced imaging techniques, such as VBM and diffusion tensor imaging, can offer critical insights into how *L*-dopa influences brain volumetric outcomes in PD, particularly regarding its impact on neural structure and the association with cognitive and olfactory function.^{50,51} In addition, the incorporation of machine learning algorithms in volumetric analysis could facilitate the identification of subtle morphometric changes that traditional VBM may overlook. Such approaches could enhance our understanding of the differential effects of treatment modalities on brain structure and function, ultimately leading to more personalized therapeutic strategies for PD treatment.

This study encountered limitations. The MRI scanning was conducted at 1.5 Tesla. Acknowledging the limitations of 1.5T MRI, higher-field strengths in 3T or 7T MRI can

significantly enhance sensitivity. The increased magnetic field strength improves the signal-to-noise ratio, leading to greater image clarity and the ability to detect smaller lesions. This could provide more in-depth results by examining cortical thickness and comparing it with brain volume.

5. Conclusion

PD patients exhibited more severe olfactory dysfunction in the hippocampal regions compared to the HC group. This may be attributed to the initial pathological loss of GM in both the right and left hippocampi.

Acknowledgments

We extend our sincere gratitude to all those who assisted us in conducting this research.

Funding

The authors are grateful for the technical assistance and financial support of Hamadan University of Medical Sciences (project code: 140203091653) and would like to thank the Clinical Research Development Unit of Hamadan University of Medical Sciences, Hamadan, Iran.

Conflict of interest

The authors declared that they have no competing interests.

Author contributions

Conceptualization: Naser Moradi

Data curation: Naser Moradi, Siamak Shahidi, Bahareh Zaker Harofteh, Ghodratollah Roshanaei

Formal analysis: Naser Moradi, Bahareh Zaker Harofteh, Ghodratollah Roshanaei

Investigation: Naser Moradi, Siamak Shahidi, Bahareh Zaker Harofteh, Mohammad Ahmadpanah, Sajjad Farashi

Methodology: Naser Moradi, Siamak Shahidi, Bahareh Zaker Harofteh, Mohammad Ahmadpanah

Writing – original draft: Naser Moradi

Writing – review & editing: Naser Moradi

Ethics approval and consent to participate

Ethical approval was obtained from Hamadan University of Medical Sciences (ethical approval: IR.UMSHA.REC.1401.1053). All participants in our study were adults, and each provided written informed consent before participation.

Consent for publication

Written informed consent was obtained from all participants to publish their data.

Availability of data

Data are available through the corresponding authors upon reasonable request.

References

- Doty RL, Deems DA, Stellar S. Olfactory dysfunction in parkinsonism: A general deficit unrelated to neurologic signs, disease stage, or disease duration. *Neurology*. 1988;38(8):1237-1244.
doi: 10.1212/WNL.38.8.1237
- Hawkes CH, Shephard BC, Daniel SE. Is Parkinson's disease a primary olfactory disorder? *Qjm Int J Med*. 1999;92(8):473-480.
doi: 10.1093/qjmed/92.8.473
- Pont-Sunyer C, Hotter A, Gaig C, et al. The onset of nonmotor symptoms in Parkinson's disease (The ONSET PD Study). *Mov Disord*. 2015;30(2):229-237.
doi: 10.1002/mds.26077
- Hummel T, Nordin S. Olfactory disorders and their consequences for quality of life. *Acta Otolaryngol*. 2005;125(2):116-121.
doi: 10.1080/00016480410022787
- Politis M, Wu K, Molloy S, Bain PG, Chaudhuri KR, Piccini P. Parkinson's disease symptoms: The patient's perspective. *Mov Disord*. 2010;25(11):1646-1651.
doi: 10.1002/mds.23135
- Munhoz RP, Moro A, Silveira-Moriyama L, Teive HA. Non-motor signs in Parkinson's disease: A review. *Arq Neuropsiquiatr*. 2015;73:454-462.
doi: 10.1590/0004-282X20150029
- Tissingh G, Berendse HW, Bergmans P, et al. Loss of olfaction in *de novo* and treated Parkinson's disease: Possible implications for early diagnosis. *Mov Disord*. 2001;16(1):41-46.
doi: 10.1002/1531-8257(200101)16:1<41:AID-MDS1017>3.0.CO;2-M
- Barresi M, Ciurleo R, Giacoppo S, et al. Evaluation of olfactory dysfunction in neurodegenerative diseases. *J Neurol Sci*. 2012;323(1-2):16-24.
doi: 10.1016/j.jns.2012.08.028
- Gottfried JA. Central mechanisms of odour object perception. *Nat Rev Neurosci*. 2010;11(9):628-641.
doi: 10.1038/nrn2883
- Kadohisa M, Wilson DA. Separate encoding of identity and similarity of complex familiar odors in piriform cortex. *Proc Natl Acad Sci U S A*. 2006;103(41):15206-15211.
doi: 10.1073/pnas.0604313103
- Staubli U, Fraser D, Kessler M, Lynch G. Studies on retrograde and anterograde amnesia of olfactory memory after denervation of the hippocampus by entorhinal cortex lesions. *Behav Neural Biol*. 1986;46(3):432-444.
doi: 10.1016/S0163-1047(86)90464-4
- Wilson DA, Xu W, Sadrian B, Courtiol E, Cohen Y, Barnes DC. Cortical odor processing in health and disease. *Prog Brain Res*. 2014;208:275-305.
doi: 10.1016/B978-0-444-63350-7.00011-5
- Jones-Gotman M, Zatorre RJ. Odor recognition memory in humans: Role of right temporal and orbitofrontal regions. *Brain Cogn*. 1993;22(2):182-198.
doi: 10.1006/brcg.1993.1033
- Zatorre RJ, Jones-Gotman M, Evans AC, Meyer E. Functional localization and lateralization of human olfactory cortex. *Nature*. 1992;360(6402):339-340.
doi: 10.1038/360339a0
- Plailly J, Howard JD, Gitelman DR, Gottfried JA. Attention to odor modulates thalamocortical connectivity in the human brain. *J Neurosci*. 2008;28(20):5257-5267.
doi: 10.1523/JNEUROSCI.5607-07.2008
- Gao Y, Nie K, Huang B, et al. Changes of brain structure in Parkinson's disease patients with mild cognitive impairment analyzed via VBM technology. *Neurosci Lett*. 2017;658:121-132.
doi: 10.1016/j.neulet.2017.08.028
- Tessitore A, Santangelo G, De Micco R, et al. Cortical thickness changes in patients with Parkinson's disease and impulse control disorders. *Parkinsonism Relat Disord*. 2016;24:119-125.
doi: 10.1016/j.parkreldis.2015.10.013
- Möller C, Hafkemeijer A, Pijnenburg YA, et al. Different patterns of cortical gray matter loss over time in behavioral variant frontotemporal dementia and Alzheimer's disease. *Neurobiol Aging*. 2016;38:21-31.
doi: 10.1016/j.neurobiolaging.2015.10.020
- Ashburner J, Friston KJ. Voxel-based morphometry--the methods. *Neuroimage*. 2000;11(6):805-821.
doi: 10.1006/nimg.2000.0582
- Chapleau M, Aldebert J, Montembeault M, Brambati SM. Atrophy in Alzheimer's disease and semantic dementia: An ALE meta-analysis of voxel-based morphometry studies. *J Alzheimers Dis*. 2016;54(3):941-955.
doi: 10.3233/JAD-160382
- Matsuda H. MRI morphometry in Alzheimer's disease. *Ageing Res Rev*. 2016;30:17-24.
doi: 10.1016/j.arr.2016.01.003
- Serra L, Cercignani M, Lenzi D, et al. Grey and white matter changes at different stages of Alzheimer's disease. *J Alzheimers Dis*. 2010;19(1):147-159.

- doi: 10.3233/JAD-2010-1223
23. Moradi N, Shahidi S, Ahmadpanah M, Farashi S, Roshanaei G. Cortical and subcortical gray matter volume and cognitive impairment in Parkinson's disease. *Appl Neuropsychol Adult*. 2024;31:1-14.
doi: 10.1080/23279095.2024.2443591
24. Taherkhani S, Moztarzadeh F, Seraj J, et al. Iran smell identification test (Iran-SIT): A modified version of the university of pennsylvania smell identification test (UPSIT) for iranian population. *Chem Percept*. 2015;8(4):183-191.
doi: 10.1007/s12078-015-9192-9
25. Gaser C, Dahnke R, Thompson PM, Kurth F, Luders E, The Alzheimer's Disease Neuroimaging Initiative. CAT: A computational anatomy toolbox for the analysis of structural MRI data. *Gigascience*. 2024;13:giae049.
doi: 10.1093/gigascience/giae049
26. Ashburner J, Friston KJ. Unified segmentation. *Neuroimage*. 2005;26(3):839-851.
doi: 10.1016/j.neuroimage.2005.02.018
27. Ashburner J. A fast diffeomorphic image registration algorithm. *Neuroimage*. 2007;38(1):95-113.
doi: 10.1016/j.neuroimage.2007.07.007
28. Lee S, Kim SS, Tae WS, et al. Regional volume analysis of the Parkinson disease brain in early disease stage: Gray matter, white matter, striatum, and thalamus. *AJNR Am J Neuroradiol*. 2011;32(4):682-687.
doi: 10.3174/ajnr.A2372
29. Halliday GM. Thalamic changes in Parkinson's disease. *Parkinsonism Relat Dis*. 2009;15:S152-S155.
doi: 10.1016/S1353-8020(09)70804-1
30. Xia J, Wang J, Tian W, et al. Magnetic resonance morphometry of the loss of gray matter volume in Parkinson's disease patients. *Neural Regen Res*. 2013;8(27):2557-2565.
doi: 10.3969/j.issn.1673-5374.2013.27.007
31. Gottfried JA, Zald DH. On the scent of human olfactory orbitofrontal cortex: Meta-analysis and comparison to non-human primates. *Brain Res Brain Res Rev*. 2005;50(2):287-304.
doi: 10.1016/j.brainresrev.2005.08.004
32. Braak H, Del Tredici K, Rüb U, De Vos RA, Steur ENJ, Braak E. Staging of brain pathology related to sporadic Parkinson's disease. *Neurobiol Aging*. 2003;24(2):197-211.
doi: 10.1016/s0197-4580(02)00065-9
33. Braak H, Bohl JR, Müller CM, Rüb U, De Vos RA, Del Tredici K. Stanley fahn lecture 2005: The staging procedure for the inclusion body pathology associated with sporadic Parkinson's disease reconsidered. *Move Disord*. 2006;21(12):2042-2051.
doi: 10.1002/mds.21065
34. Silveira-Moriyama L, Holton JL, Kingsbury A, et al. Regional differences in the severity of Lewy body pathology across the olfactory cortex. *Neurosci Lett*. 2009;453(2):77-80.
doi: 10.1016/j.neulet.2009.02.006
35. Li Y, Xu J, Liu Y, et al. A distinct entorhinal cortex to hippocampal CA1 direct circuit for olfactory associative learning. *Nat Neurosci*. 2017;20(4):559-570.
doi: 10.1038/nn.4517
36. Bohnen NI, Gedela S, Herath P, Constantine GM, Moore RY. Selective hyposmia in Parkinson disease: Association with hippocampal dopamine activity. *Neurosci Lett*. 2008;447(1):12-16.
doi: 10.1016/j.neulet.2008.09.070
37. Roh H, Kang J, Koh SB, Kim JH. Hippocampal volume is related to olfactory impairment in Parkinson's disease. *J Neuroimaging*. 2021;31(6):1176-1183.
doi: 10.1111/jon.12911
38. Barrett MJ, Murphy JM, Zhang J, et al. Olfaction, cholinergic basal forebrain degeneration, and cognition in early Parkinson disease. *Parkinsonism Relat Disord*. 2021;90:27-32.
doi: 10.1016/j.parkreldis.2021.07.024
39. Patel R, Stebbins G, Bernard B, Goldman J. Hippocampal and entorhinal cortex atrophy across the Parkinson's disease cognitive impairment spectrum (S39.004). *Neurology*. 2017;88(16-Suppl):S39.
doi: 10.1212/WNL.88.16-supplement.S39.004
40. Frisoni GB, Laakso MP, Beltramello A, et al. Hippocampal and entorhinal cortex atrophy in frontotemporal dementia and Alzheimer's disease. *Neurology*. 1999;52(1):91-91.
doi: 10.1212/wnl.52.1.91
41. Iizuka N, Masaoka Y, Kubota S, et al. Entorhinal cortex and parahippocampus volume reductions impact olfactory decline in aged subjects. *Brain Behav*. 2021;11(5):e02115.
doi: 10.1002/brb3.2115
42. Kubota S, Masaoka Y, Sugiyama H, et al. Hippocampus and parahippocampus volume reduction associated with impaired olfactory abilities in subjects without evidence of cognitive decline. *Front Human Neurosci*. 2020;14:556519.
doi: 10.3389/fnhum.2020.556519
43. Bitzenhofer SH, Westeinde EA, Zhang HXB, Isaacson JS. Rapid odor processing by layer 2 subcircuits in lateral entorhinal cortex. *Elife*. 2022;11:e75065.
doi: 10.7554/eLife.75065
44. Sun Y, Jin S, Lin X, et al. CA1-projecting subiculum neurons facilitate object-place learning. *Nat Neurosci*. 2019;22(11):1857-1870.

- doi: 10.1038/s41593-019-0496-y
45. Chen YN, Kostka JK, Bitzenhofer SH, Hanganu-Opatz IL. Olfactory bulb activity shapes the development of entorhinal-hippocampal coupling and associated cognitive abilities. *Curr Biol.* 2023;33(20):4353-4366.e5.
doi: 10.1016/j.cub.2023.08.072
46. Donzuso G, Sciacca G, Rascunà C, *et al.* Structural MRI substrate of long-duration response to levodopa in Parkinson's disease: An exploratory study. *J Neurol.* 2021;268:4258-4264.
doi: 10.1007/s00415-021-10550-5
47. Kaur K, Gill JS, Bansal PK, Deshmukh R. Neuroinflammation - a major cause for striatal dopaminergic degeneration in Parkinson's disease. *J Neurol Sci.* 2017;381:308-314.
doi: 10.1016/j.jns.2017.08.3251
48. Vivekanantham S, Shah S, Dewji R, Dewji A, Khatri C, Ologunde R. Neuroinflammation in Parkinson's disease: Role in neurodegeneration and tissue repair. *Int J Neurosci.* 2015;125(10):717-725.
doi: 10.3109/00207454.2014.982795
49. Araújo B, Caridade-Silva R, Soares-Guedes C, *et al.* Neuroinflammation and Parkinson's disease-from neurodegeneration to therapeutic opportunities. *Cells.* 2022;11(18):2908.
doi: 10.3390/cells11182908
50. Ielo A, Bonanno L, Brunati C, *et al.* Structural and functional connectomics of the olfactory system in Parkinson's disease: A systematic review. *Parkinsonism Relat Disord.* 2024;132:107230.
doi: 10.1016/j.parkreldis.2024.107230
51. Georgiopoulos C, Warntjes M, Dizdar N, *et al.* Olfactory impairment in Parkinson's disease studied with diffusion tensor and magnetization transfer imaging. *J Parkinsons Dis.* 2017;7(2):301-311.
doi: 10.3233/JPD-161060